Optical-Model Description of Low-Energy Collisions Between Heavy Ions

J. A. KUEHNER AND E. ALMQVIST
Chalk River Nuclear Laboratories, Chalk River, Ontario, Canada
(Received 16 January 1964)

An optical model has been used to describe the elastic scattering of $O^{16}+C^{12}$, $N^{14}+C^{12}$, and $N^{14}+Be^{9}$ for energies near and above the Coulomb barrier. Using a Woods-Saxon form for both the real and imaginary potentials, good agreement with the experimental data is obtained. Quantitative differences between $O^{16}+C^{12}$, which exhibits well-developed diffraction structure, and the other two systems, which exhibit less pronounced diffraction structure, are well accounted for by the model and mainly reflect differences in the size of the imaginary potential, a small imaginary potential being associated with the large amplitude diffraction oscillation. The parameters determined by fitting the elastic scattering data yield reaction cross sections in agreement with measured data. Although the model gives a good description of the data there are difficulties in the physical interpretation which arise from the deep interpenetration of the colliding ions implied by the model; for $O^{16}+C^{12}$, which requires a small absorption in order to fit the large diffraction oscillations, the mean free path inside the potential is $\sim$6 F. Such a deep interpenetration does not seem physically realistic, yet, within the framework of the model it appears to be a necessary condition for producing the observed amplitude of diffraction oscillations.

A. INTRODUCTION

THE advent of the tandem accelerator a few years ago, for the first time made possible studies of heavy-ion elastic scattering at precisely defined energies in the energy range near the top of the Coulomb barrier and such studies[1–3] have revealed some very interesting new features. In some cases, sharp resonances are observed, in others a broad diffraction-like structure is seen, and in other cases only a smooth featureless energy dependence is found. These different features are apparent in Fig. 1. The $O^{16}+C^{12}$ scattering exhibits sharp resonance structure ($\sim$200 keV wide) as well as suggesting a broader (2–3 MeV wide) structure; the $N^{14}+Be^{9}$ scattering on the other hand has a smooth, nearly monotonic, energy dependence. Even at energies within one or two MeV of the "break" from pure Coulomb scattering, where the two cases shown in Fig. 1 both appear to have a similar smooth energy dependence, there are marked differences in the angular dependence of the elastic scattering cross sections. This fact is illustrated in Fig. 2; here the angular distribution of the $O^{16}+C^{12}$ case shows a diffraction-like structure in contrast again to a smooth monotonic angular variation of the $N^{14}+Be^{9}$ elastic scattering. This paper deals primarily with an attempt to see whether a simple optical-model potential for the nucleus-nucleus interaction can account for the broad features of the elastic scattering—particularly the differences in the angular distributions of the type shown in Fig. 2 which occur near the Coulomb barrier energy. However, the object was not only to find a systematic set of potential parameters that would fit the elastic interactions of a number of nucleus-nucleus systems but also to obtain a plausible set of potentials for the purpose of computing transmission factors that are required in compound-nucleus calculations of heavy-ion cross sections. These calculations are the subject of a separate paper that is in preparation.

The attempt made in this paper to account for the average features of the low-energy nucleus-nucleus scattering uses a complex interaction potential of the Woods-Saxon type. Since the optical model cannot be expected to account for the sharp resonance structure which appears at higher energies in the $O^{16}+C^{12}$ case

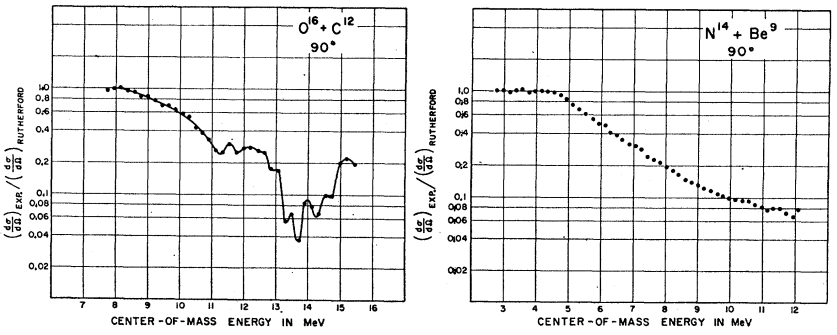

FIG. 1. The energy dependence of the elastic scattering at 90° in the center-of-mass system of O^{16} by C^{12} at the left and of N^{14} by Be^{9} at the right. The ordinate is the observed scattering cross section divided by the Rutherford cross section.

[1] D. A. Bromley, J. A. Kuehner, and E. Almqvist, Phys. Rev. Letters 4, 365 (1960); D. A. Bromley, J. A. Kuehner, and E. Almqvist, Phys. Rev. **123**, 878 (1961).
[2] J. A. Kuehner, E. Almqvist, and D. A. Bromley, Phys. Rev. **131**, 1254 (1963).
[3] J. A. Kuehner and E. Almqvist, Bull. Am. Phys. Soc. **6**, 48 (1961); and to be published.

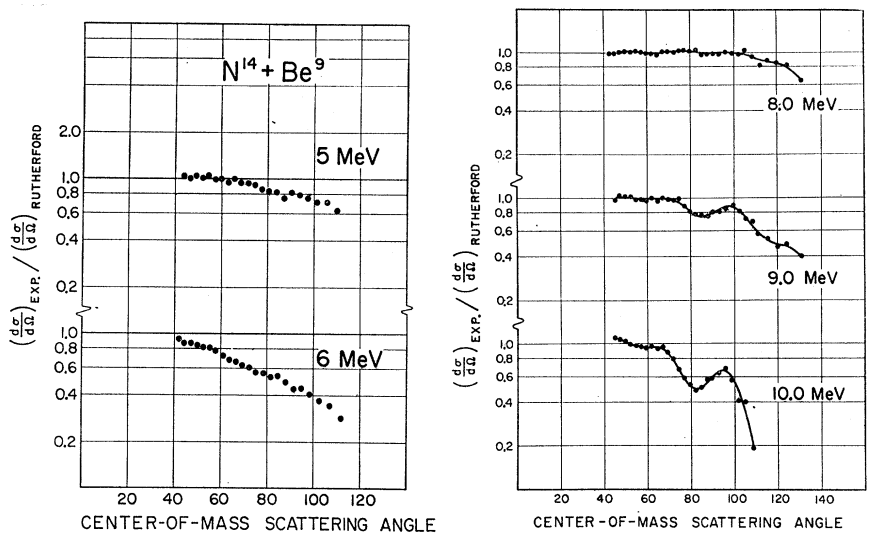

FIG. 2. Angular distributions for the elastic scattering of N^{14} by Be^{9} at the left and of O^{16} by C^{12} at the right. The ordinate is the observed scattering cross section divided by the Rutherford cross section.

as well as in other systems, most notably in $C^{12}+C^{12}$, only low-energy data were considered initially. In addition a simple interaction potential might be expected *a priori* to apply successfully to distant collisions in which only interpenetration of the low-density outermost nucleons might be expected. In fact the optical-model fits obtained even at low energies are shown below to imply greater interpenetration of the nuclei than seems physically reasonable. The potentials obtained were used to compute transmission factors and total absorption cross sections which are compared with experimental values.

B. THE OPTICAL-MODEL POTENTIAL

Calculations were carried out using an existing program[4] and a Burroughs 205 (Datatron) computer. In these calculations numerical solutions are found for the Schrödinger equation with a complex potential.

$$V(r)=V(r)_{\text{Coulomb}}+V(r)_{\text{nuclear}}+(\hbar^2/2\mu)[l(l+1)/r^2].$$

The Coulomb potential used was that for a uniformly charged sphere of radius R_c. The nuclear potential, which is complex, used a Woods-Saxon form[5] and can be written

$$V(r)_{\text{nuclear}}=(V_0+iW_0)/\{1+\exp[(r-R_0)/a]\}.$$

Since the model parameters, R_c, V_0, W_0, R_0, and a, are five in number, and since no automatic search routine was available, it was felt desirable to reduce the number of parameters. Consequently, R_c was set equal to R_0 in all calculations. The relation

$$R_0=r_0(A_1^{1/3}+A_2^{1/3})$$

was used to define a reduced radius r_0; A_1 and A_2 are the mass numbers of the incident and target nuclei.

Reasoning that the reflection at the potential surface should be at least as important for heavy ions as in the case of alpha-particle scattering, where Igo[6] was able to show that the scattering is dependent mainly on the surface of the optical-model potential, it was decided initially to fix V_0 at -50 MeV and thus to reduce the number of parameters to three. As is discussed later, this procedure is justified, since, for the cases considered, it appears that the scattering can determine at most only two parameters of the real potential well.

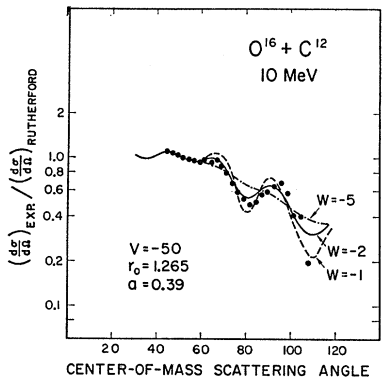

FIG. 3. The curves are the results of optical-model computations with three different values of the imaginary potential depth W. The points are experimental data for $O^{16}+C^{12}$ scattering at 10 MeV.

C. FITS TO THE DATA

Since only three parameters are involved, the fits were obtained by observing trends as one parameter at a time was changed. In this way sets of parameters that gave reasonably good fits to all the low-energy data were found. As will be discussed in the following section D the fits do not comprise a unique set of parameters.

The effect of varying the imaginary part of the potential, W, while holding the remaining parameters

[4] J. M. Kennedy, Chalk River Report CRT-1052, 1961 (unpublished).

[5] R. D. Woods and D. S. Saxon, Phys. Rev. **95**, 577 (1954).

[6] G. J. Igo, Phys. Rev. Letters **1**, 72 (1958); Phys. Rev. **115**, 1665 (1959).

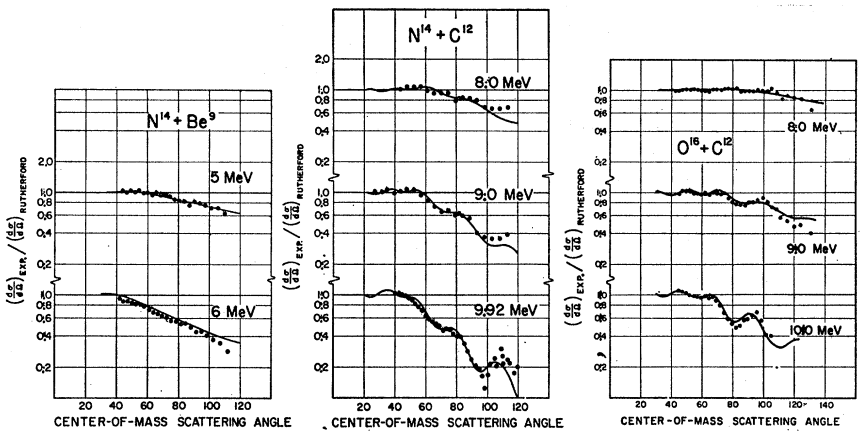

FIG. 4. The curves are optical-model fits to the experimental data for $N^{14}+Be^{9}$ at the left, $N^{14}+C^{12}$ in the middle, and $O^{16}+C^{12}$ at the right. The optical-model parameters are: $N^{14}+Be^{9}$; $V=-50$ MeV, $W=-10$ MeV, $r_0=1.31$ F, $a=0.45$ F. $N^{14}+C^{12}$; $V=-50$ MeV, $W=-4$ MeV, $r_0=1.19$ F, $a=0.49$ F. $O^{16}+C^{12}$; $V=-50$ MeV, $W=-2$ MeV, $r_0=1.265$ F, $a=0.39$ F.

constant is demonstrated in Fig. 3 for the $O^{16}+C^{12}$ system at 10 MeV. A small value of W is seen to produce a large "diffraction" oscillation and a large value results in an almost smooth curve. It is apparent in Fig. 4, which shows the fits obtained to the experimental results for three different systems, that it is, indeed, mainly this one difference, the size of W, that distinguishes the different cases; the values of W are -10, -4, and -2 MeV for the $N^{14}+Be^{9}$, $N^{14}+C^{12}$, and $O^{16}+C^{12}$ systems, respectively.

The remaining parameters, r_0 and a, while not affecting the size of the oscillations affect the positions of the peaks and valleys. In fact, it is possible to cause these peaks and valleys to move to larger or smaller angles until a new and approximately equally good fit is obtained by appropriate changes in r_0 and a. This ambiguity is discussed more fully in the following section D.

The measured behavior of the elastic scattering at 90° as a function of the energy for the $O^{16}+C^{12}$ and the $N^{14}+Be^{9}$ systems is compared in Fig. 5 to the optical-model calculations. The latter are based on the parameters which yield a fit to the angular distributions at low energy shown in Fig. 4. The three curves in the $O^{16}+C^{12}$ case correspond to three possible fits obtained to the low-energy angular distributions using three different combinations of r_0 and a, as discussed above and in more detail below. As expected, the three calculated curves agree very well with each other in the region from 8 to 10 MeV where the angular distributions were fitted; for the higher energies the different cases give somewhat different results, possibly allowing a choice among them to be made. However, all three cases predict a broad dip at about 13 MeV, consistent with a qualitative trend of the data if one averages over the narrow resonance structure.

In the $N^{14}+Be^{9}$ case, the energy dependence of the data is smooth and it is possible to obtain a very good fit. The different curves are in this case for different values of W, and give an indication of the degree to which this parameter is determined. The curve with $W=-10$ MeV corresponds to the fit shown for the low-energy angular distributions in Fig. 4.

It is suggested by the curves shown in Figs. 3, 4, and

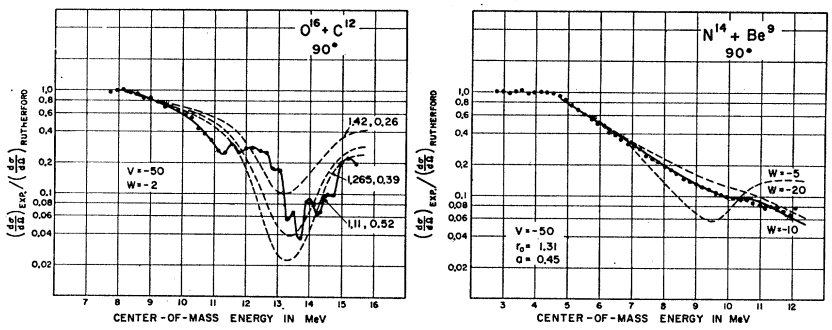

FIG. 5. The dashed curves on the left were computed using the sets of parameters that fit the low-energy $O^{16}+C^{12}$ angular distributions in Fig. 4; the solid curve in this case has no significance but to join the experimental points. The solid curve through the $N^{14}+Be^{9}$ data on the other hand is the result of an optical-model computation using the parameters determined by fitting the corresponding angular distributions in Fig. 4; the dashed curves show the effect of varying the magnitude of the imaginary potential W.

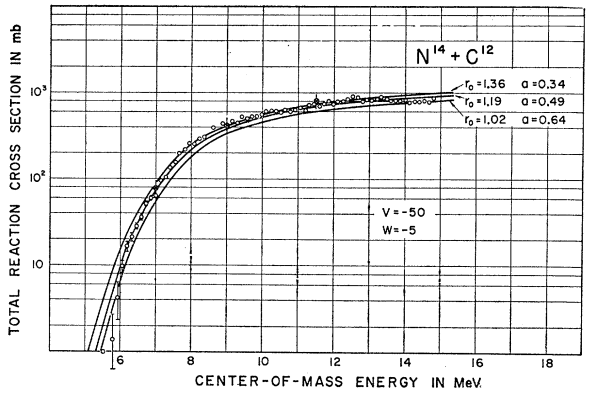

FIG. 6. Total reaction cross section data for $N^{14}+C^{12}$. The curves are the results of optical-model computations using the parameters determined by the fits to the elastic scattering. Both the absolute scale and the shapes of the curves are in good agreement with the experimental points.

5 and is borne out by detailed inspection of the optical-model phase shifts which is discussed in the following sections that the diffraction oscillations of the angular distributions are a result of size resonances. When W is increased, these size resonances get broader until they completely overlap and disappear.

Figures 6 and 7 compare the optical-model prediction for the reaction cross section with some recent measurements.[7] The data points in Figs. 6 and 7, consisting of crosses, represent measurements of charged particles integrated over all angles. Small corrections for the undetected neutron emission and three-particle breakup have been included. The open points are the results of measurements in which essentially all pulses from a 3×3-in. NaI scintillation detector placed at 90° to the beam were recorded. Since most reaction channels result in one or more gamma rays, this method yields a fair measure of the energy dependence of the total

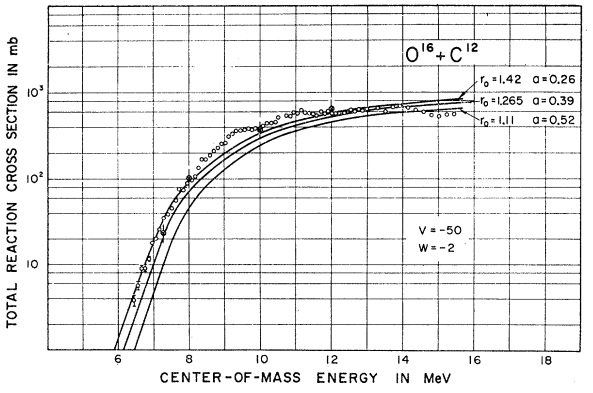

FIG. 7. Total reaction cross section data for $O^{16}+C^{12}$. The curves are the results of optical-model calculations using the parameters determined by the fits to the elastic scattering. Both the absolute values and the trend of the cross sections are in fair agreement with the experimental points.

[7] E. Almqvist and J. A. Kuehner (to be published).

reaction cross section. These gamma-ray data are used to interpolate and extrapolate the yield curves between and beyond the few points shown by crosses where absolute cross sections were measured. The three calculated curves in each case correspond to three possible fits to the low-energy elastic scattering angular distributions. Apart from a suggestion of local irregularities in the $O^{16}+C^{12}$ case, which might be interpreted as a size resonance effect in the region of 8 to 12 MeV, the optical model correctly predicts the reaction cross sections.

D. DISCUSSION

Figure 8 summarizes the optical-model parameters obtained for the three scattering systems considered. The sets of points in the (r_0,a) plane for $O^{16}+C^{12}$ and $N^{14}+C^{12}$ correspond to sets of parameters which give satisfactory fits to the data. In each case it is the middle point which corresponds to the fit shown in Fig. 4. The

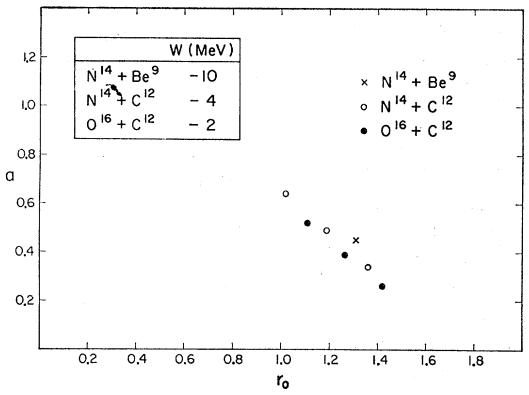

FIG. 8. The optical-model parameters obtained from fitting the elastic scattering data are summarized. Values of r_0 and a are plotted and values of W are listed in the inset table. In all cases a value of V equal to -50 MeV was used. These parameters and the potential used are defined in the text of Sec. B.

position in the (r_0,a) plane on a line at right angles to the sets of points shown, i.e., on a line given approximately by $r_0=a+0.8$, appears to be most closely related to the effects usually associated with the nuclear size; motion along this line in the direction of increasing r_0 and a increases the average deviation from Rutherford scattering, as well as increasing the reaction cross section, while motion perpendicular to the line mainly affects the positions of the oscillations. It appears, therefore, that only small differences in the nuclear size exist between the different systems, apart from the $A_1^{1/3}+A_2^{1/3}$ factor in the interaction radius.

The (r_0,a) ambiguity revealed in this work, in which satisfactory fits to the data can be obtained with a discrete set of values of r_0 and a, is similar to the well-depth ambiguity discussed by Adair[8] for neutron

[8] R. K. Adair, Phys. Rev. 94, 737 (1954).

scattering and to the $V-W$ ambiguity for deuteron scattering discussed recently by Drisko *et al.*[9]

Figure 9 gives an example of the ambiguity for $O^{16}+C^{12}$ scattering. The data points give the experimental angular distribution at 10 MeV. Of the three curves, those labeled *a* and *c* correspond to two adjacent regions in the (r_0,a) plane where satisfactory fits were obtained. The curve labeled *b*, which has its "diffraction" pattern obviously displaced, used values of r_0 and a which are the arithmetic mean of those used for curves *a* and *c*.

In attempting to understand why the ambiguity illustrated in Fig. 9 occurs, it is instructive to examine the details of the optical model calculation. In Fig. 10 are plotted the magnitude and phase of the "reflection coefficients" η_l. [The η_l are complex quantities calculated in the optical-model program and are related to the optical-model phase shifts σ_l by $\eta_l=\exp(2i\sigma_l)$]. It

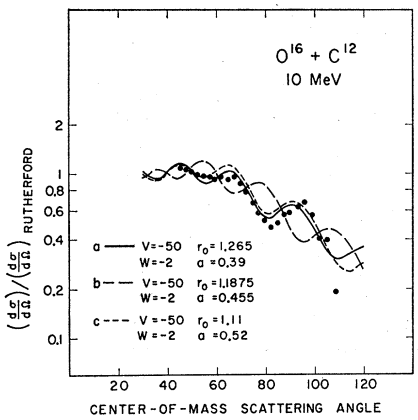

FIG. 9. Optical-model curves for three different potentials are compared with the $O^{16}+C^{12}$ scattering angular distribution at 10 MeV. The curves labeled *a* and *c* correspond to two sets of optical-model parameters which both give good fits to the experimental data. The curve labeled *b* uses optical-model parameters which are the arithmetic mean of those used for curves *a* and *c* and does not fit the experimental data.

is strongly suggested by the nature of the curves in Figs. 9 and 10 that the diffraction oscillations in the angular distributions are related to coherent effects in the reflection coefficients in which there is a periodic change in both modulus and phase in going from even to odd values of l. It is seen that solutions *a* and *c* show periodic effects in η_l which are in phase with each other but out of phase with those of solution *b*.

This result follows from the fact that the changes in the potential involved are just of the correct magnitude to allow exactly one less node in the radial wave function in going from solution *a* to solution *c*. This is illustrated in Fig. 11, which shows the modulus of the radial wave function for $l=0$ and $l=7$ for each of the cases labeled *a* and *c* in Figs. 9 and 10.

[9] R. M. Drisko, G. R. Satchler, and R. H. Bassel, Phys. Letters **5**, 347 (1963).

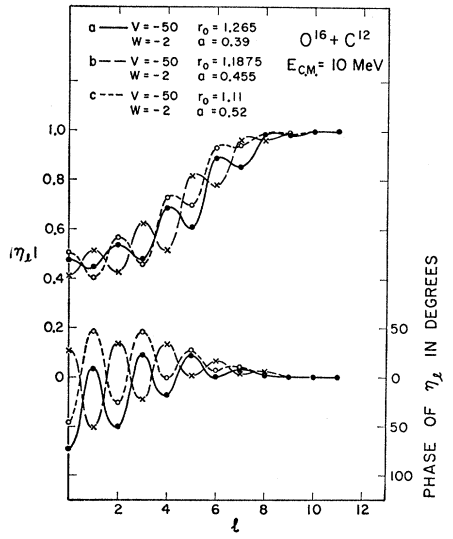

FIG. 10. The modulus and phase of the reflection coefficient η_l are plotted as a function of l for three cases. The curves labeled *a* and *c* correspond to two sets of optical-model parameters which give very nearly the same elastic scattering (see curves *a* and *c* of Fig. 9). The parameters used for case *b* are the arithmetic mean of those cases *a* and *c* (see also Fig. 9).

It is clear that the even-odd periodicity illustrated in Fig. 10 is a manifestation of "size-resonance effects, i.e., the effects of a potential exactly the correct size to

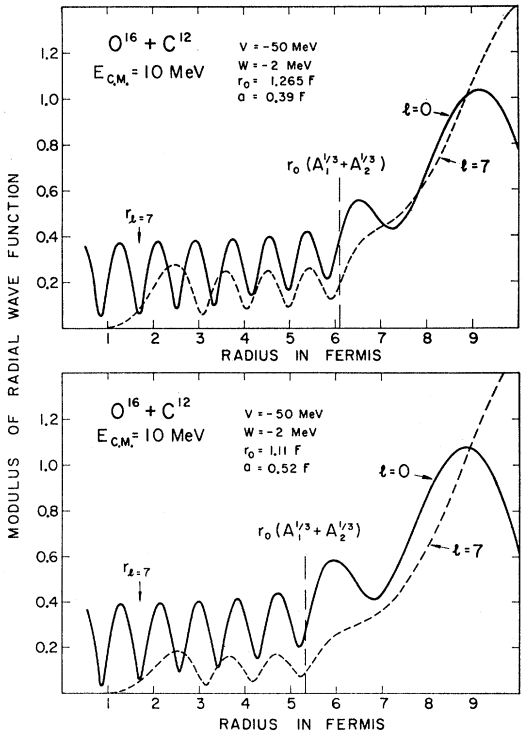

FIG. 11. The modulus of the radial wave functions are plotted against the radius for $l=0$ and 7 partial waves for the cases *a* (top) and *c* (bottom) of Figs. 9 and 10. The positions of the angular momentum barrier for $l=7$ partial waves, $r_{l=7}$, and of the half-value point of the nuclear potential, $r_0(A_1^{1/3}+A_2^{1/3})$, are indicated.

accommodate the required number of nodes of the radial-wave function for each partial wave. An earlier assertion is now made more clear, namely, that the diffraction oscillations observed in the elastic scattering angular distributions have the same essential origin as the size resonances in the energy distribution.

As pointed out by Drisko *et al.*[9] using results derived in the WKB approximation by Austern,[10] the condition for ensuring that one more wave be contained inside the potential becomes apparent from the expressions for the WKB phase shifts

$$\eta_l = \exp[2iS_l(r_l)].$$

Here

$$S_l(r_l) = C_l + \int_{r_l}^{\infty} K_l(r)dr,$$

where

$$K_l(r) = (2\mu/\hbar^2)^{1/2} \times [E_{\text{c.m.}} - V(r) - V_c(r) - iW(r) - (\hbar^2/2\mu r^2)l(l+1)]^{1/2}.$$

C_l is a constant and r_l is the classical turning point nearest the origin. It is seen that if the difference $S_{l'}(r_l) - S_l(r_l)$ (where the primed and unprimed symbols refer to two different potentials) is π or an integral number times π then the η_l are unaffected. For the potentials a and c $S_{0'}(r_0) - S_0(r_0)$ is $2.73 + 0.06i$. The difference between this number and π may well arise mainly in the barrier region due to a breaking down of the WKB validity condition

$$|(dK_l/dr)/2K_l^2| \ll 1.$$

It is seen from the small imaginary part of the above difference that the values of $S_l(r_l)$ obtained from the above relations are quite insensitive to W for the potentials used in this paper. Since the positions of the diffraction oscillations in the angular distributions are apparently determined approximately by the $S_l(r_l)$ it follows that their positions should not be sensitive to changes in W. This is indeed the case (see Fig. 3).

It was pointed out above, in connection with Fig. 5, that one might be able to resolve the ambiguity between the various solutions by making use of the energy dependence data. However, this would require energy independence of the potential, a condition which is usually not assumed to hold.

McIntosh *et al.*[11] theoretically obtain the long-range part of the interaction between N^{14} and C^{12} from the nucleon-nucleus optical-model potential. Their calculations suggest that values of $a \sim 0.5$ would be appropriate for the $N^{14} + C^{12}$ potential. However, even if the value of the surface thickness parameter a were fixed, there would still be an ambiguity of the type discussed above (i.e., the undetermined number of nodes), since V_0 and r_0 could be adjusted to allow more or fewer nodes in the wave functions.

While the real potential appears to control the number of nodes of the wave function inside the nucleus the imaginary potential has very little effect in this regard. Instead, the imaginary potential controls the size of the diffraction oscillations. Let us now turn to a consideration of the significance of the imaginary potential.

The inset table in Fig. 8 summarizes the values of W obtained. Physically it appears reasonable that in low-energy collisions W should be largest for those cases involving loosely bound nucleons that can readily be transferred from one nucleus to the other. Such transfer processes will result in absorption from the incident beam in distant collisions and, on this point of view, scattering involving Be^9 would be expected to have a larger W than $O^{16} + C^{12}$ collisions, where both nuclei are strongly bound, in agreement with the results of the optical-model fits.

However, examination of Fig. 3 reveals that the main effect of a small W is a prominent diffraction structure in the elastic scattering angular distribution. This leads to the question: What specifically within the framework of the model makes a small value of W lead to large diffraction effects? In order to gain some insight into this question, it is instructive to examine in detail the optical-model phase shifts and wave functions for cases with differing values of W. In Fig. 12 are plotted the modulus and phase of the reflection coefficient η_l for the cases $W = -2$ MeV (closed circles) and $W = -5$ MeV (open circles) corresponding to two of the angular distribution curves of Fig. 3. The first point to notice is that for this low-energy case there is no small region

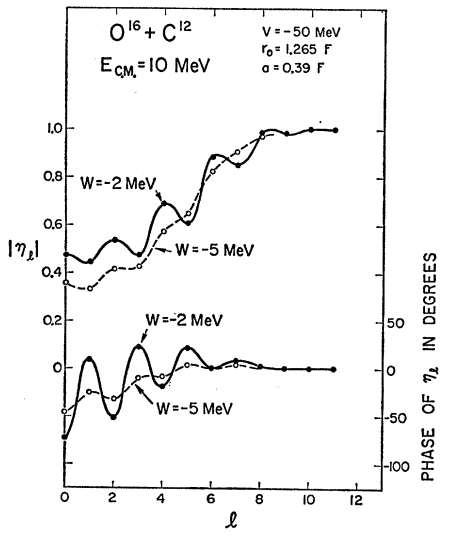

FIG. 12. The modulus and phase of the reflection coefficients η_l are plotted as a function of l for the cases $W = -2$ MeV (closed circles) and $W = -5$ MeV (open circles) corresponding to two of the angular distribution curves of Fig. 3.

[10] N. Austern, Ann. Phys. (N. Y.) **15**, 299 (1961).

[11] J. S. McIntosh, S. C. Park, and G. H. Rawitscher (to be published). See also *Proceedings of the Second Conference on Reactions between Complex Nuclei*, edited by A. Zucker, F. T. Howard, and E. Halbert (John Wiley & Sons, Inc., New York, 1960).

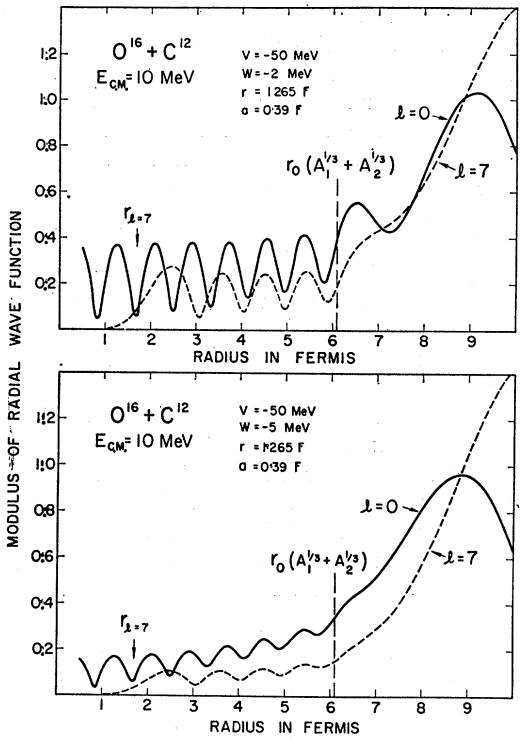

FIG. 13. The modulus of the radial wave functions are plotted against the radius for $l=0$ and 7 partial waves for $W=-2$ MeV (top) and for $W=-5$ MeV (bottom), corresponding to two of the angular distribution curves of Fig. 3.

of l corresponding to the transition from $|\eta_l|$ small to $|\eta_l|=1$. One can therefore expect important contributions from all partial waves below about $l=8$. Secondly, both the modulus and phase of η_l oscillate with a period $\sim 2l$, the oscillation being smaller in amplitude for the larger value of W. It has been pointed out by Austern[10] that this oscillation results from interference between the waves reflected at the surface and those reflected at the centrifugal barrier (well inside the potential for this low-energy case). Thus, for W sufficiently small (such that the mean free path is of the order of the interaction radius), this interference causes an oscillatory behavior of both modulus and phase of η_l, resulting in systematic differences in η_l for odd and even values of l. This, in turn, leads to an oscillatory angular distribution since the Legendre functions making up the amplitude for scattering add in a coherent manner.

The mean free path in an optical potential can be written[12]

$$\text{mfp}=(4.6/\mu^{1/2})[(E-V)^{1/2}/-W],$$

where μ is the reduced mass, $E-V$ is the kinetic energy, and W is the imaginary potential. Strong oscillations appear with $W=-2$ MeV, for which the mean free path is ~ 6.8 F. With $W=-5$ MeV, the mean free path is reduced to ~ 2.7 F, thus allowing only a small fraction of the incident wave to penetrate to the angular momentum barrier; the result is a very weak interference oscillation.

Figure 13 contains graphs of the modulus of the radial wave function for the $l=0$ and 7 partial waves for $W=-2$ MeV (top) and for $W=-5$ MeV (bottom). The positions of the surface, equal to $r_0(A_1^{1/3}+A_2^{1/2})$, and of the angular momentum barrier for $l=7$, defined by equating the kinetic energy in the potential to the angular momentum energy for $l=7$, are indicated in Fig. 13. As expected, the amplitude of the wave function inside the potential is considerably larger for the case of the smaller absorption and indeed remains large in to a radius less than 1 F.

Now, a question arises: Is it physically realistic for a C^{12} nucleus to penetrate an O^{16} nucleus to the extent of 4 to 5 F overlap, without being absorbed? It appears, at first sight, that this is not realistic and that the correct interpretation may be that the optical model happens to give the correct phase shifts but for the wrong reasons. A more realistic model might involve nuclear distortions at close approach with a resultant rearrangement barrier preventing deep interpenetration or possibly it might involve the resonant transfer of an alpha particle[13] in the case of $O^{16}+C^{12}$.

It should be pointed out that a similar situation exists in the case of alpha-particle scattering. In order to demonstrate this fact a correlation was looked for between the observed amplitudes of diffraction structure in alpha-particle scattering and the mean-free path divided by the distance from the surface to the angular momentum barrier. This is shown in Fig. 14. The data shown are those tabulated by McIntyre *et al.*[14] The

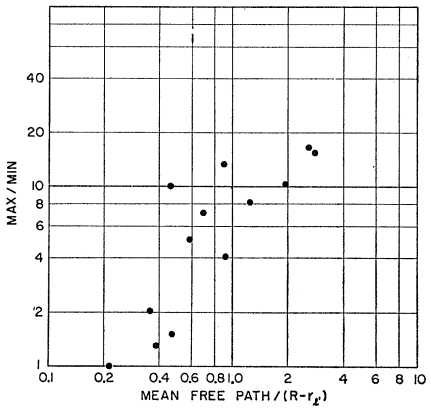

FIG. 14. The observed average amplitude of the diffraction oscillations for alpha-particle elastic scattering from a number of elements is plotted as a function of the mean free path divided by the distance from the interaction radius to the position of the angular momentum barrier.

[12] F. L. Friedman and V. F. Weisskopf, *Neils Bohr and the Development of Physics*, edited by W. Pauli (McGraw-Hill Book Company, Inc., New York, 1955).

[13] G. Temmer, Phys. Letters **1**, 10 (1962).

[14] J. A. McIntyre, S. D. Baker, and T. L. Watts, Phys. Rev. **116**, 1212 (1959).

ordinate is the observed average ratio of cross section on a maximum to that in a minimum. The abscissa was calculated using published[6] optical-model parameters. The interaction radius R was set equal to $1.17(A)^{1/3}+1.77$ and $r_{l'}$ was calculated by equating the kinetic energy inside the potential to the angular momentum energy. The value of l' was determined by equating the kinetic energy to the angular momentum energy at the interaction radius, R. Figure 14 suggests an interpretation of the optical-model fits to the alpha-particle scattering data which is similar to that outlined above for $O^{16}+C^{12}$ scattering. Thus, if the mean free path is made large with respect to the distance from the surface to the angular momentum barrier then large diffraction oscillations are obtained. Of course an alpha particle might reasonably have a much larger mean free path inside the nucleus than a more massive structure such as a C^{12} nucleus.

E. SUMMARY

Satisfactory quantitative fits to a number of heavy-ion elastic scattering angular distributions measured for energies near the Coulomb barrier have been obtained using an optical model. Taking the parameters determined by these low-energy fits, it is found that the model gives a good account of the behavior of the elastic scattering as a function of collision energy up to energies as high as twice the Coulomb barrier value and also gives quantitative agreement with total reaction cross-section measurements over this same energy range. This agreement suggests that the given potentials can be used at low energies to compute reliable transmission factors which are required in compound nucleus computations of heavy-ion reactions.

The model is able to account for the diffraction structure that sometimes occurs in heavy-ion elastic scattering. This structure is shown to have the same origin as the size resonances in the energy distributions. The positions of the oscillations are found to be sensitive to the real potential in a way which is related to the number of nodes of the radial wave functions which are contained in the potential. The amplitudes of the diffraction oscillations are found to be dependent on the magnitude of the imaginary potential; this magnitude determines the amount of the wave function which can penetrate through the nuclear potential to be reflected by the angular momentum barrier and return to give rise to interference effects at the surface. For the case of $O^{16}+C^{12}$ scattering, a mean free path inside the optical-model potential of ~ 6 F is required to account for the observed diffraction oscillations. Such deep interpenetration does not seem physically realistic, yet, within the framework of the model it appears to be a necessary condition for producing the observed amplitude of diffraction oscillations.

In conclusion it should be emphasized that there is no really compelling evidence that actual physical heavy ions interpenetrate to great depths when undergoing nuclear collisions. If such deep interpenetration does not take place then one must regard the optical model for these cases as being simply a convenient parameterization of the data with little or no further physical significance.

ACKNOWLEDGMENT

The authors are indebted to E. W. Vogt for many stimulating discussions.